T.C.
ISTANBUL OKAN UNIVERSITY
INSTITUTE OF GRADUATE SCIENCES

THESIS

FOR THE DEGREE OF

MASTER OF SCIENCE

IN AUTOMOTIVE MECHATRONICS AND INTELLIGENT VEHICLES PROGRAM

Hani DUMLU

(193005014)

DESIGN AND IMPLEMENTATION OF RESIDUAL CURRENT SENSOR FOR ELECTRIC VEHICLE CHARGING SYSTEMS

THESIS ADVISOR

Assoc. Prof. Dr. Ömer Cihan KIVANÇ

ISTANBUL, February 2023

T.C.
ISTANBUL OKAN UNIVERSITY
INSTITUTE OF GRADUATE SCIENCES

THESIS FOR THE DEGREE OF MASTER OF SCIENCE IN AUTOMOTIVE MECHATRONICS AND INTELLIGENT VEHICLES PROGRAM

Hani DUMLU
(193005014)

DESIGN AND IMPLEMENTATION OF RESIDUAL CURRENT SENSOR FOR ELECTRIC VEHICLE CHARGING SYSTEMS

Date Thesis Delivered to Institute: February 13, 2023
Date of Thesis Defense: February 13, 2023
Thesis Advisor: Assoc. Prof. Dr. Ömer Cihan KIVANÇ

Jury Members: Prof. Dr. Ramazan Nejat TUNCAY

Assoc. Prof. Dr. Salih Barış ÖZTÜRK

ISTANBUL, February 2023

ABSTRACT

DESIGN AND IMPLEMENTATION OF RESIDUAL CURRENT SENSOR FOR ELECTRIC VEHICLE CHARGING SYSTEMS

With the increasing use of electric vehicles, the infrastructure of charging stations has also expanded. As a result, it is observed that direct current (DC) and alternative current (AC) charging stations are also becoming widespread. AC charging stations (or equipment), which consist of a relay that disconnects the circuit, and a signal called a control pilot, also contain a residual current sensor (RCD) as per the automotive regulations and standards. These residual current sensors connect the grid from the vehicle when a residual current of 30 mA AC, 6 mA DC using flux gate type sensors. Although this equipment can measure with high linearity, sensitivity, and accuracy, they also have high current consumption. They consist of a saturated inductance placed on a toroidal magnetic core and a signal processing circuit. The most important feature of the residual current sensor is that they have low saturation current, low inductance value, high permeability, and small volume size. Flux gate type sensors come to the fore, especially since the nano-crystalline softcore material has very high permeability and low power loss. Various types of sensing circuits have been seen in the literature and the market. As most companies design their integrated circuits (IC) and microcontrollers (MCU), the need for a suitable toroid design and an advanced signal processing circuit has been identified. For this reason, a sensor with a self-oscillating circuit, high sensitivity, and an oscillator circuit that detects imbalances in the flowing current has been developed within the thesis's scope. In this thesis, the toroid is designed and analyzed using ANSYS Maxwell for appropriate B-H curve and inductance value. An oscillator circuit with a microprocessor is designed and implemented for the signal-processing circuit using Altium. The prototyped sensor has been performed on commercial electric vehicle. As a result of the experimental studies, the developed system is verified for 6 mA DC, 30 mA AC residual current.

Keywords: Self Oscillation, Residual Current Sensor, Electric Vehicle, Charge System, Signal Processing, Finite Element Method

KISA ÖZET

ELEKTRİKLİ ARAÇ ŞARJ SİSTEMLERİ İÇİN KAÇAK AKIM SENSÖRÜ TASARIMI VE GERÇEKLEMESİ

Artan elektrikli araç kullanımı ile şarj istasyonu altyapısı da genişlemektedir, Bununla birlikte DA ve AA şarj istasyonlarının da yaygınlaşması gözlenmektedir. Temelde akım akan tüm iletkenlerin bağlantısını kesen bir röle ve control ve pilot sinyallerinden oluşan AA şarj istasyonları aynı zamanda standartlar gereği bir de kaçak akım sensörü barındırmaktadırlar. Bu kaçak akım sensörleri 30 mA AA, 6 mA DA ve üzeri kaçak akım oluştuğunda şebekenin araçla bağlantısını kesme işlevine sahiptirler. Bu kaçak akımları algılayabilmek için *"flux-gate"* tipi sensörler kullanılmaktadır. Bu donanımlar yüksek lineerlik, yüksek hassasiyet ve doğruluk ile ölçüm yapabilmelerine karşın yüksek akım tüketimine de sahiptirler. Bu sensörler doyumlu bir endüktansın toroidal bir manyetik çekirdek üzerine yerleştirilmesi ve bir sinyal işleme devresinden oluşmaktadırlar. Kaçak akım sensörünün en önemli özelliği düşük satürasyon akımı, düşük endüktans ve yüksek geçirgenlik ile küçük hacimli boyuta sahip olmalarıdır. Özellikle nano-kristalin yumuşak çekirdek materyali çok yüksek geçirgenliğe ve düşük güç kaybına sahip olduğu için *"flux-gate"* tipi sensörler öne çıkmaktadır. Literatürde ve pazarda farklı tipte algılama devreleri yer almaktadır. Çoğunlukla firmaların kendi çiplerini vee işlemcilerini tasarlaması sebebiyle uygun bir toroid tasarımı ve gelişmiş bir sinyal işleme devresine olan ihtiyaç tespit edilmiştir. Bu sebeple tez kapsamında kendinden osilasyonlu bir devreye, yüksek hassasiyetli ve akımdaki bozulmaları tespit eden bir osilatör devresine sahip bir sensör geliştirilmiştir. Toroid tasarımı ANSYS Maxwell ile geliştirilmiş ve sonlu elemanlar metodu ile analiz edilmiştir. Toroidin B-H eğrisine ve endüktans değerine analiz sonucunda ulaşılmıştır. Sinyal işleme devresi için mikroişlemciye sahip bir osilatör devresi Altium ile tasarlanmıştır. Geliştirilen kaçak akım sensörü elektrikli bir araç üzerinde test edilmiştir. Testler sonucunda 6 mA DA, 30 mA AA kaçak akım uygulanarak geliştirilen sistem doğrulanmıştır.

Anahtar Kelimeler: Kendinden Osilasyon, Kaçak Akım Sensörü, Elektrikli Araç, Şarj Sistemi, Sinyal İşleme, Sonlu Elemanlar Yöntemi

ACKNOWLEDGMENT

I wish to express my deepest gratitude and appreciation to my supervisor Assoc. Prof. Dr. Ömer Cihan Kıvanç for his continuous support during my M.Sc. study and related work, and for his patience and motivation. His helpful and valuable suggestions, as well as his continuous encouragement, have contributed significantly to the completion of this thesis.

This work was supported by The Scientific and Technological Research Council of Turkey (TUBITAK) (grant 121E412). Therefore, I am grateful to TUBITAK for its support in supplying the hardware parts via the national support programme of TUBITAK 1002.

TABLE OF CONTENTS

PAGE NO

LIST OF FIGURES

PAGE NO

LIST OF TABLES

PAGE NO

ABBREVIATIONS

EV: Electric Vehicle

HPV: Hydrogen Powered Vehicle

ICE: Internal Combustion Engines

DC: Direct Current

AC: Alternating Current

IEC: International Electrotechnical Commission

RCD: Residual Current Protection Device

LPF: Low Pass Filter

PLL: Phased Lock Loop

LVDC: Low Voltage Direct Current

IC: Integrated Circuit

MCU: Microcontroller

SO-FGS: Self Oscillating Flux Gate Sensor

EVSE: Electric Vehicle Supply Equipment

DSP: Digital Signal Processor

I. INTRODUCTION

1.1. Overview

The increasing demand for energy and the growing negative environmental effects of conventional energy production have transformed the approach to electric power generation. In recent years, significant progress has been made in renewable energy [1]. Especially, the air pollution caused by conventional energy generation techniques has played a major role in the rapid development of renewable energy generation techniques such as photovoltaics [2]. Moreover, due to their high emissions during energy generation, traditional internal combustion engine (ICE) transportation vehicles are being replaced by electric vehicles (EV) and hydrogen (HPV) powered vehicles [2]. Hence, it has been determined that more than 10 million electric vehicles have replaced conventional transportation vehicles globally, which means an increase of 41% compared to previous years [3]. Replacing traditional methods, modern methods of energy generation and transportation have brought about large-scale development in power electronics [4].

Electric vehicle sales are rapidly increasing globally in recent years, thanks to policies that support different types of electric vehicles and charging infrastructure. At the end of 2018, the total number of electric vehicles in the global vehicle stock exceeded 5 million. Projections show that the total number of electric vehicles worldwide could reach between 120 and 250 million by 2030 [36]. In response to these developments, Turkey has recently started to develop its own market with around 1000 electric vehicles in use. However, with the increase in vehicle ownership and population growth, there is significant potential for the use of electric vehicles to increase. In addition, Turkey has accelerated its efforts towards domestic electric vehicle production soon. This acceleration also brings the production of auxiliary equipment for electric

vehicles. The leading equipment among these are charging cables, portable type-2 charging systems, type-2, type-3 wall-mounted charging stations, and DC fast charging stations [32]. A typical electric vehicle is delivered to the user with a type-2, mode-3 charging cable and portable charging equipment in both Turkey and European countries. In addition, apartment, charging station, shopping mall, and wall-mounted chargers suitable for personal use are also available. These devices require IEC 62752 control and protection devices for mode-2 charging of electric vehicles, and a 62995-leakage direct current monitoring sensor is mandatory [37]. According to new regulations, both 30 mA AC and 6 mA DC leakage current monitoring equipment are required for both portable and wall-mounted charging systems. Additionally, AC/DC leakage current relays are needed to protect both the vehicle and the user during charging, as required by IEC 62955 and IEC 60364 standards. The high cost of using separate AC and DC leakage current sensors has led to the development of sensors that can detect both types of current within the same hardware. However, there are only a few companies producing these sensors, and they are currently priced between 40 and 70 dollars.

There are numerous methods and products available for measuring AC leakage currents, there are fewer options available for measuring DC leakage currents. This is particularly important for electric vehicles, which have high-voltage battery packs that can leak DC current. IEC 62752 standards have mandated the need for monitoring 6 mA of DC leakage current. However, many of the products currently available on the market are only designed to measure AC leakage current, and there is a need for sensors that can detect both AC and DC leakage current.

IEC 62752 standards, provide fault signals for both 30 mA AC and 6 mA DC leakage current up to 400 V and 3 phases x 40 A, perform its own external testing, and provide a frequency range of up to 2 kHz. The basic principle of leakage current sensors is based on applying a square wave to a toroidal primary and secondary winding and analyzing the resulting

symmetric/asymmetric current. When leakage current flows, the symmetry is disrupted, and the Fourier analysis of the signal determines the magnitude of the leakage current. If the magnitude is 6 mA or greater, the output signal triggers the relay to open. While there are some leakage current sensors available for signal processing, there is currently no compact design with advanced communication capabilities that complies with IEC 62752 for electric vehicle charging systems.

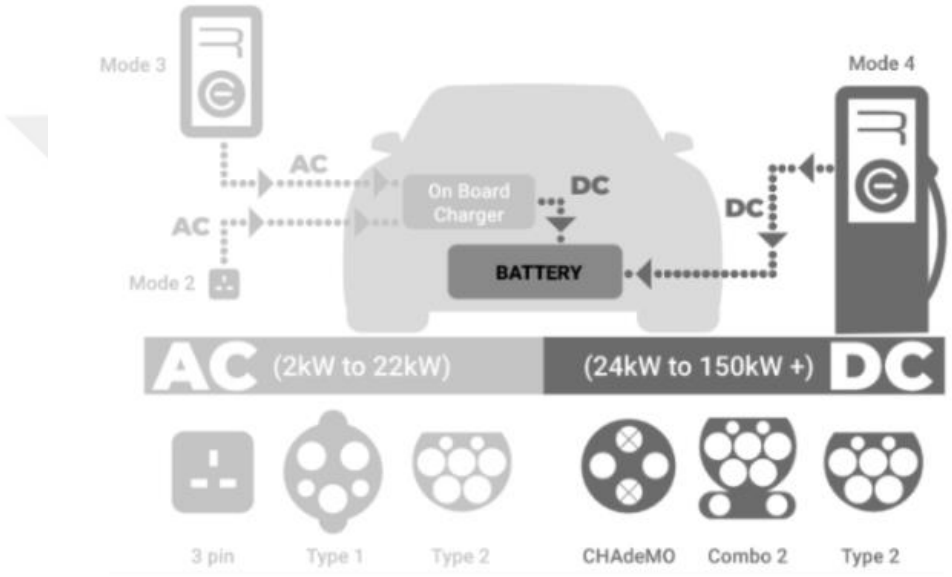

Figure I.1. Electric vehicle charger ecosystem.

1.2. Residual Current Sensor Types

Although alternating current (AC) is still the prevalent form of electrical energy used today, the development of direct current (DC) powered electronic devices, battery storage systems, wind turbines, and photovoltaic systems has accelerated significantly [4]. The fact that the energy produced in photovoltaic systems is DC and electric vehicles are charged with DC energy are examples of this rapid improvement. Photovoltaic systems and EV charging systems contain AC and DC circuits. To utilize the energy generated in photovoltaic systems, it is required to use DC-AC power electronic converters. These converters are known as "inverter" in the literature. Different topology types have been provided in the literature for these

converters. Single-phase converters for low-power applications [5-7], three-phase converters for medium and high-power applications [8-11] and multi-level converters for high-resolution applications [12-14] have been proposed in the literature and analyzed in terms of grounding techniques [15].

As mentioned earlier, the development of DC-powered electronic devices has brought about the development of a wide range of DC current measurement techniques. The general purpose of the rapid development of DC current measurement techniques may be listed as power management in systems requiring DC, development of feedback control mechanisms, online surveillance, and protection. In recent years, with the increasing use of electronic devices, among other things, protecting people against electrical hazards has become a major concern. In particular, the failure of unwanted residual currents to leave the system safely due to grounding faults has been one of the leading electrical hazards. In general, the resistance in earthing cables is chosen to be low to allow residual current to pass through the system, but if the cable is damaged, the current seeks an alternative path for passage. In such a case, the human body provides an alternative path for the current [16]. Residual current can damage the human body and even cause death. In addition, residual current increases the risk of fire in low-voltage circuits. Fuses are known as the first protective circuit element to be used in electrical circuits. Due to their inability to react quickly to high currents that may occur in case of a short circuit, switches have been used as circuit breaker elements in electrical circuits. Thanks to their internal structure, switches provide protection against overloads by interrupting the circuit in case of temperature increases that occur in short circuit situations. However, switches cannot provide any protection against residual currents. As a solution to this problem, residual current sensors (RCD) are proposed and used in the literature. In the standards, residual current sensors are analyzed in four different types according to detection capacities. An AC-type residual current sensor is used to detect residual currents with a frequency of 50/60 Hz and a sinusoidal

waveform. The AC-type residual current sensor does not detect the DC components of the residual current. A type A residual current sensor, just as the type of AC, is used to detect residual currents with a frequency of 50/60 Hz and a sinusoidal waveform. In addition to the AC type, it detects the DC components of the residual current with a maximum 6 mA measuring range. Type F residual current sensor has similar characteristics to type A. However, the measuring range is 6 mA in type A while it is 10 mA in type F. Type B, another residual current sensor, is used to detect residual currents with sinusoidal waveforms up to 1000 Hz. In addition to other types, it is also used to detect residual currents with mixed frequency [2].

Power electronics circuits such as rectifiers, inverters, and filters are also used in electric vehicle charging stations. As with other electrical hazards, there is a risk of residual current when a grounding fault occurs in the charging station. Together with the rapidly evolving charging methods, high-power (>80 kW) charging stations have been put into service around the world. Thus, researchers have started to widely investigate high-power electric vehicle charging stations [17-19]. With such an increased interest in charging stations, the safety of charging stations against electrical hazards has become an important research topic. Standard no. IEC62752 of the International Electrotechnical Commission has become a safety standard for manufacturers of electric vehicle charging stations. Residual current protection in charging stations is quite like other applications. However, due to the rapid development in the sector and the governmental regulations for the protection of nature, residual current protection sensors in charging stations have gained particular importance.

1.3. Literature Survey

Nowadays, the IEC62752 standard requires charging stations to have a type B residual current sensor for the detection of residual current. A type B residual current sensor can detect DC residual currents at different frequencies. In the literature, researchers have proposed different circuit designs for the measurement of DC current, one of which is the “Self-

Oscillating Fluxgate Based Semi-Digital Sensor for DC High Current Measurement" [20]. This technology uses the RL-multivibrator, as proposed by Filanovsky and Piskarev [21], in combination with a nonlinear transformer and a comparator [22].

Afterwards, Pross et al. [23] developed a nonlinear model [24] by using simulation and experimental methods (and in later stages, based on the "ArcTan" function), and a linearity of 1.2% for ±250A is obtained. With reference to these technologies, residual current sensors have also been developed and included in the literature [25, 26]. According to the findings, the best accuracy is better than 0.5%, but the measurable current range is only ±10A [27]. To improve these methods, increase the measurement range, and improve accuracy, an integrator was added to enable DC flux compensation in the core [28] and a pulse width modulated feedback circuit significantly reduced power dissipation. In this way, linearity can be improved by up to 0.1% in the ±20A measurement range, but circuit complexity and cost increase [29].

The measurement principles of this type of sensor are based on the measurement of the average excitation current and the primary current. To obtain the average current, a low-pass filter (LPF) is needed. Furthermore, to increase the measurement range, the core needs to be deeply saturated [30]. In this case, the waveform of the excitation current has a large slope. This distortion in the waveform of the excitation current causes design difficulties and increased costs.

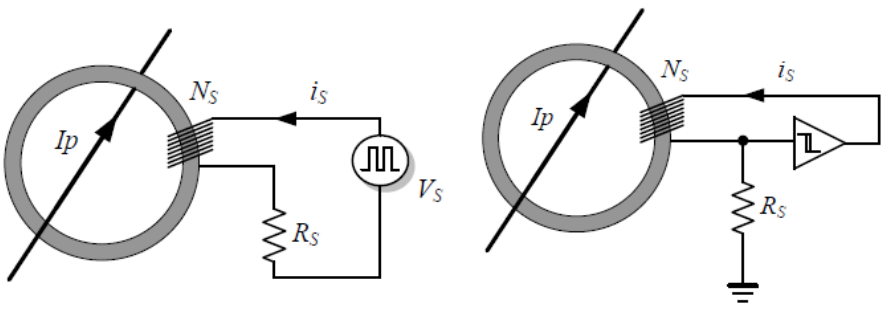

Figure I.2. Diagram of conventional and self-oscillating open-loop fluxgate sensors [4].

On the other hand, a self-oscillating fluxgate-based circuit that can solve these problems is presented in the literature [23]. This circuit is based on measuring the exciter voltage and primary current. The relationship between the two has been verified by researchers through simulation and experimental methods [31, 32], but no theoretical equations have been found to describe the linear dependence between them. Moreover, in these studies, the analog and complex nature of the circuit measuring the duty cycle of the pulse signal limited the maximum measurable linear range to ±2A.

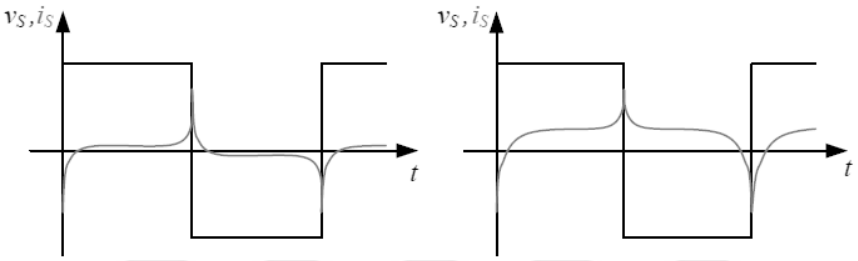

Figure I.3. Excitation waveforms [4].

Sensor sensitivity, accuracy, and resolution have not been emphasized so far in the literature. Researchers achieved a maximum linear measurement range of ±750 A in DC current measurements with a self-oscillating fluxgate-based semi-digital DC high current measurement sensor. A microcontroller unit is used in this sensor structure, which is based on the duty cycle of the pulse signal determined by a simple waveform generator circuit. Furthermore, researchers presented a precise theoretical equation showing the relationship between the pulse signal's duty cycle and the current.

In summary, a self-oscillating circuit-based residual current sensor is a type of device that uses an oscillator circuit to detect and respond to imbalances in the current flowing between live and neutral conductors in an electrical circuit. The circuit is designed in a way that when the live and neutral currents are equal, the oscillator will be in a steady state and there will be no output signal. But when there is an imbalance in the live and neutral currents, the oscillator becomes unstable and produces an output signal that is used to trigger the residual current

sensor and cut power to the circuit. The self-oscillating circuit is designed by using a switching element such as a comparator, a flip-flop, and a transistor. The comparator compares the live and neutral currents and if there is an imbalance, it sends a signal to the flip-flop, which triggers the switching element to turn off power to the circuit. This type of residual current sensor is useful for detecting small current leakages and can be designed to have a fast-tripping time. The self-oscillating circuit-based residual current sensor for AC residual current works similarly to a self-oscillating circuit-based residual current sensor for DC residual current, but with some key differences.

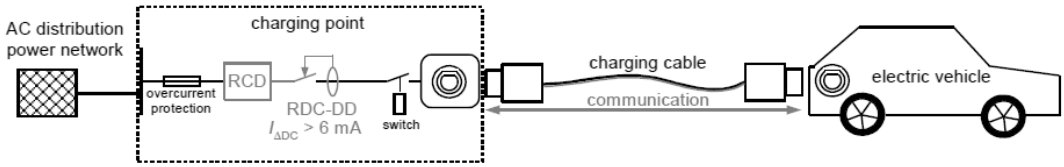

Figure I.4. Residual current device system for charging of EVs [2].

In an AC residual current sensor, the live and neutral conductors carry alternating currents that are constantly changing direction. The self-oscillating circuit should be able to detect imbalances in the current flowing between live and neutral conductors, even if the direction of the current is constantly changing. One way to achieve this is to use a full-wave rectifier circuit to convert the AC current into a unidirectional DC current, which can be easily compared with the comparator circuit in the residual current sensor. The comparator compares the rectified live current with the rectified neutral current and if there is an imbalance, it sends a signal to the flip-flop, which triggers the switching element to turn off power to the circuit. Another way is to use a zero-crossing comparator that detects the zero-crossing point of the current and compares the live and neutral current at the zero-crossing point; if there is any imbalance, the switching element is triggered to turn off power to the circuit. Such residual current sensors are useful for detecting both large and small current leaks and can be designed to have a fast-tripping time. It is possible to connect the output of a self-oscillating circuit-based residual

current sensor to a microcontroller to detect residual current. The self-oscillating circuit is designed to generate a digital output signal when an imbalance in current is detected. This digital output signal is then connected to a digital input pin on the microcontroller. The microcontroller is programmed to continuously monitor the state of the digital input pin and respond when the signal changes from a low state to a high state, indicating that an imbalance in current has been detected. The microcontroller then takes the appropriate action, such as triggering a relay or TRIAC to cut power to the circuit, or sending a signal to another device to indicate that an imbalance has been detected. Using a microcontroller in this way provides additional functionality and flexibility in RCD design. For example, the microcontroller can be programmed, for users' convenience, to set the trip threshold, trip time, and other parameters of the device or to provide remote monitoring and control capabilities. In addition, a microcontroller can also provide diagnostic and troubleshooting capabilities as it can record and store current imbalance events.

II. DESIGN STUDIES

In [4], the proposed RCD uses a Hall effect sensor to measure the residual current in LVDC power distribution systems. The Hall effect sensor is a magnetic field sensor that can detect the magnetic field generated by the current flowing through a conductor. The RCD is designed to be small, compact, and low-cost, making it suitable for use in LVDC power distribution applications. The design process of the RCD, including the selection of the Hall effect sensor, the circuit design, and the calibration of the sensor. The RCD is designed to measure residual currents up to 10A, which is sufficient for LVDC power distribution applications. The proposed RCD is evaluated experimentally to determine its accuracy and performance. The results show that the RCD can accurately measure residual currents in LVDC power distribution systems. The RCD has a low measurement error and a high sensitivity, making it suitable for use in safety-critical applications.

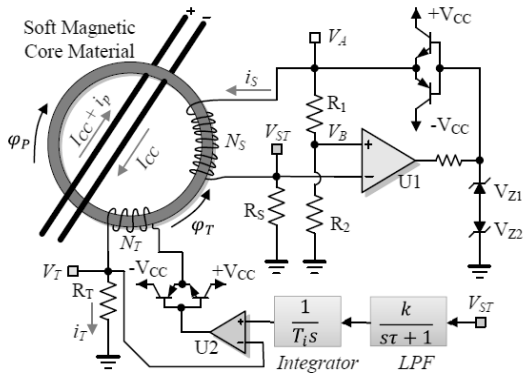

Fig. 3. Proposed residual current sensor.

Figure II.1. Proposed RCD structure in [4].

In [4], self-oscillating flux gate sensor (SO-FGS) is a type of magnetic sensor that utilizes a magnetic core and feedback circuitry to generate self-oscillations, which are used to detect the electrical current. This type of sensor is commonly used in power electronics, electric vehicles, and renewable energy systems.

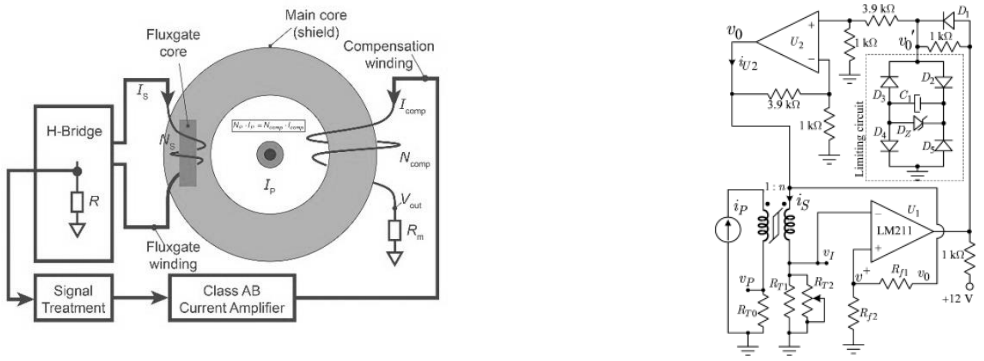

(a) (b)

Figure II.2. RCD sensor topologies, (a) LEM Company CDSR 0.07-NP [39] (b) current sensor without filtering stage [24].

The standard current sensors are based on a Hall element placed in the air gap of a transformer core and are suitable for measuring both DC and AC currents with typical accuracy between 0.5% and 2%. However, improved current sensor types based on the fluxgate principle are highly sensitive and suitable for DC measurements. Recent progress in soft magnetic materials and a decline in electronic component prices have made fluxgate current sensors economically comparable to Hall element-based sensors. The commercially available closed-loop, second harmonic-based fluxgate current sensors can measure currents in the frequency range from DC to more than 10 kHz, with accuracy ranging from 1 ppm to 0.1%. On the other hand, simplified, self-oscillating fluxgate current sensors are suitable for applications that require lower measuring performance. Although open-loop self-oscillating sensors are simple in construction, there is no satisfactory model for accurate design of sensor parameters. In this paper, an analytical model of the basic open-loop sensor based on continuous approximation of the core curve is proposed, which accurately predicts the accuracy, linearity, and other parameters that affect sensor operation. In [20], the proposed nonlinear model of the SO-FGS is developed based on the differential equations that describe the sensor's behavior. The model considers the nonlinearities in the feedback circuit and magnetic core, which can affect the sensor's accuracy and sensitivity. The model also considers the effects of temperature, bias

current, and external magnetic fields on the sensor's performance. The proposed nonlinear model of the SO-FGS can be used to optimize the sensor's performance and design parameters. The model provides a more accurate and comprehensive understanding of the sensor's behavior, which can lead to improvements in its accuracy, sensitivity, and robustness. Further research is needed to validate the model experimentally and to explore its applications in various electrical current measurement systems.

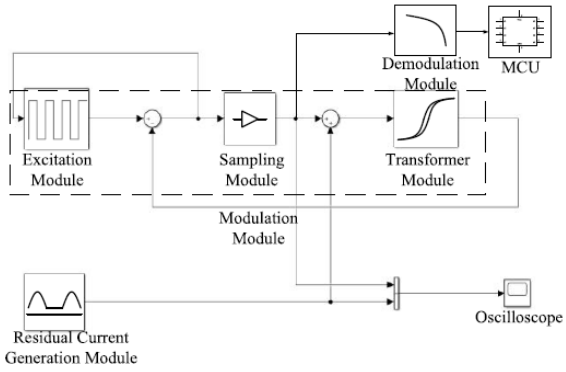

Figure II.3. Schematic diagram of DC RCD [1].

For the design and implementation of a self-oscillating fluxgate-based quasi-digital sensor for DC high-current measurement. The sensor is designed for high-precision and high-sensitivity DC current measurement in industrial applications, such as electric vehicles, renewable energy systems, and power electronics.

Table II.1. Comparison of residual current detection methods [1].

Detection method	Method type	Residual current detection type	Detection bandwidth	Detection accuracy	Response speed	Temperature drift& zero drift	Cost
electromagnetic current transformer detection method	open-loop	ac	10Hz~20kHz	a bit high	fast	a bit small temperature drift, a bit large zero drift	quite low
Hall detection method	open-loop	ac, dc	0~200kHz	a bit low	a bit fast	a bit large temperature drift, a bit large zero drift	a bit low
	close-loop			a bit low	a bit slow	a bit large temperature drift, a bit small zero drift	
giant reluctance detection method	open-loop	ac, dc	0~1MHz	a bit low	a bit fast	a bit large temperature drift, a bit large zero drift	a bit high
	close-loop			a bit high	a bit slow	a bit large temperature drift, a bit small zero drift	
magnetic modulation detection method	current type	ac, dc	0~10kHz	a bit high	a bit fast	small temperature drift, large zero drift	high
	voltage type			high	a bit fast		a bit high

The basic principles of fluxgate sensors and their advantages in high-precision DC current measurement. The article then presents the design of the self-oscillating fluxgate-based sensor, which includes a fluxgate core, an oscillator, a phase-locked loop (PLL), and a digital signal processing (DSP) unit. The fluxgate core measures the magnetic field generated by the current, and the oscillator generates a high-frequency signal that drives the fluxgate core. The PLL locks the oscillator frequency to the resonant frequency of the fluxgate core, and the DSP unit processes the signal and converts it to a digital output.

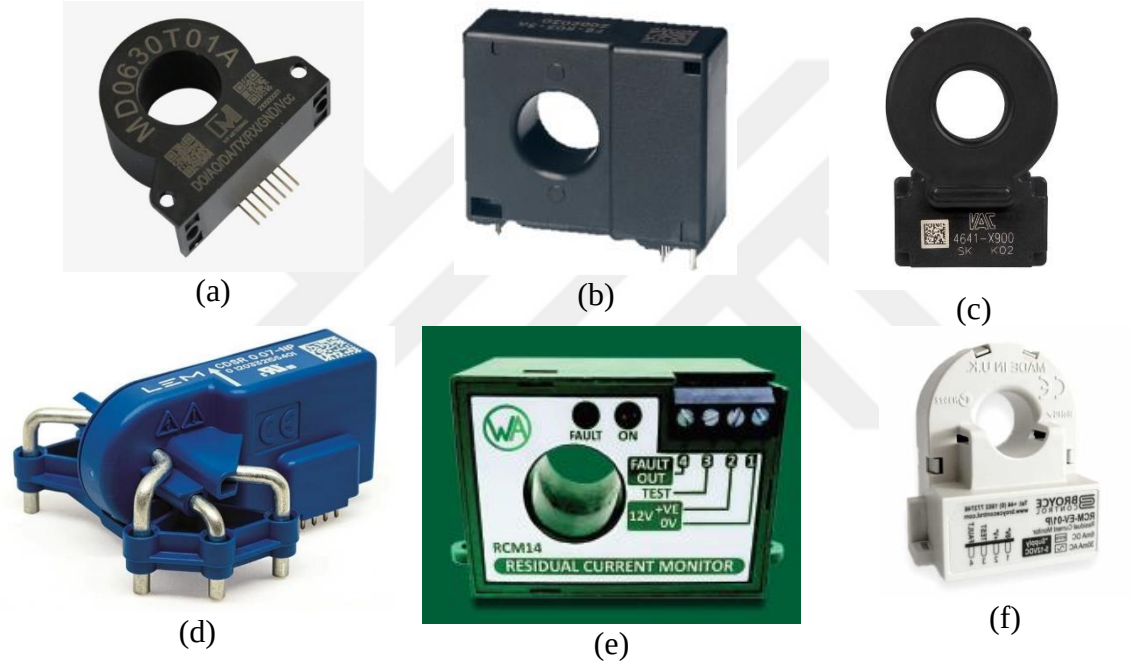

(a) (b) (c)

(d) (e) (f)

Figure II.4. RCD sensors producer in the market, (a) IVY-Metering, (b) KEMET, (c) Vacuumschmelze, (d) LEM, (e) Western Automation, (f) Broyce Control.

Isolated DC current sensors use either Hall-effect or fluxgate technology. Fluxgate transducers are more accurate but larger and consume more power. The standard form of a fluxgate transducer uses a toroidal magnetic core with a saturable inductor inside, but there is also a variation with no airgap. The measure current flows through a single-turn primary winding, while the secondary winding is referred to as the excitation coil and composes an RL circuit along with a shunt resistor. The RL circuit is excited by a square wave voltage source, and the system is designed so that the excitation current waveform is symmetric when the

primary current is zero. However, if the primary current is non-zero, an asymmetric current waveform is produced, and the second harmonic is proportional to the magnitude of the measured current. A signal processing circuit can be used to extract this information and provide an output voltage proportional to the measured current.

Flux-gate type sensors can be used to detect these residual currents. They can measure with high linearity, high precision, and accuracy, but they also have high current consumption. They are basically formed by placing a saturated inductance on a toroidal magnetic core. Low saturation current and low inductance lead to high relative permittivity and low size. Since the nano-crystalline soft-core material provides very high transmittance and low power dissipation, the fluxgate type current sensor structure is preferred in the thesis. As part of the proposed project, the KEMET FG-R05-3A sensor currently available on the market is first dissected and analyzed in detail. In addition, another commonly used leakage current sensor, the Western Automation RCM14 model, is also analyzed.

In addition, the sensor also includes a toroid mechanical casing, a sensor mechanical casing, and epoxy. The KEMET product has a double-wound toroid and consists of a signal processing circuit and an ASIC processor. In addition, the analysis of the second product, the RCM14, is shown in Figure II.4. Western Automation has launched a microprocessor-controlled sensor on the market using a more expensive structure. In commonly used sensors, current measurement sensors consist of a primary coil from the magnetic core and a secondary coil as an excitation coil. An RL circuit and a shunt resistor are also used. The RL circuit is excited by a square wave voltage source. The system increases the inductance current to a certain current value in each half cycle. Thus, saturation of the magnetic core is ensured. If the primary current is zero and symmetrical, the saturation current density of the magnetic core and the excitation current waveform are also symmetrical. However, if the primary coil current is greater than zero, a magnetic field deviation occurs, and an asymmetric waveform appears. The excitation voltage

measured here is amplified by the signal processing circuit and harmonic information is analyzed. However, these processes require demodulation of the excitation current and harmonic analysis, resulting in a costly sensor. On the other hand, the excitation voltage is passed through the RL circuit using a self-generated oscillating signal. As the signal oscillates, an unstable state is analyzed, and an asymmetric wave is generated. The signal is measured using a low-pass filter located at the output. The measured signal amplitude determines the DA and AA leakage current values and sends a signal to open the output.

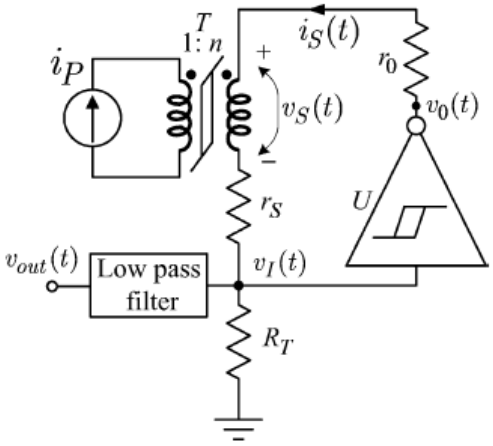

Figure II.5. Basics self-oscillating sensor circuit [24].

In residual current sensors, the excitation circuit is designed to periodically saturate the selected magnetic core. A self-oscillating structure is preferred because it provides a possibility to fulfill this request.

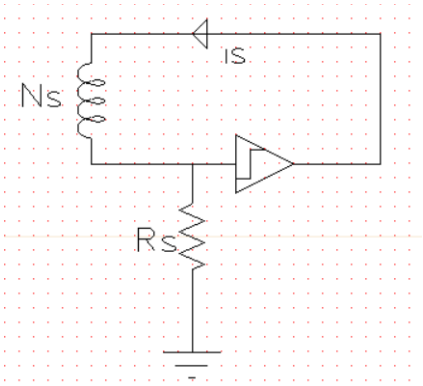

Figure II.6. Self-oscillation structure.

Basically, this structure consists of a Schmitt-trigger comparator and an *RL* circuit. The inverter Schmitt-trigger circuit is converted into a self-oscillating structure to form an astable multivibrator. As the residual current flows through the conductor in the toroid, the symmetrical structure is broken and the current flows in proportion to the residual current I_p. Measurement is made with a low-pass filter over the R_s resistor and the voltage value and residual current are proportioned. In the case of high residual current, the non-linear characteristic of the B-H curve of the inductance steps in, resulting in a weak linearity.

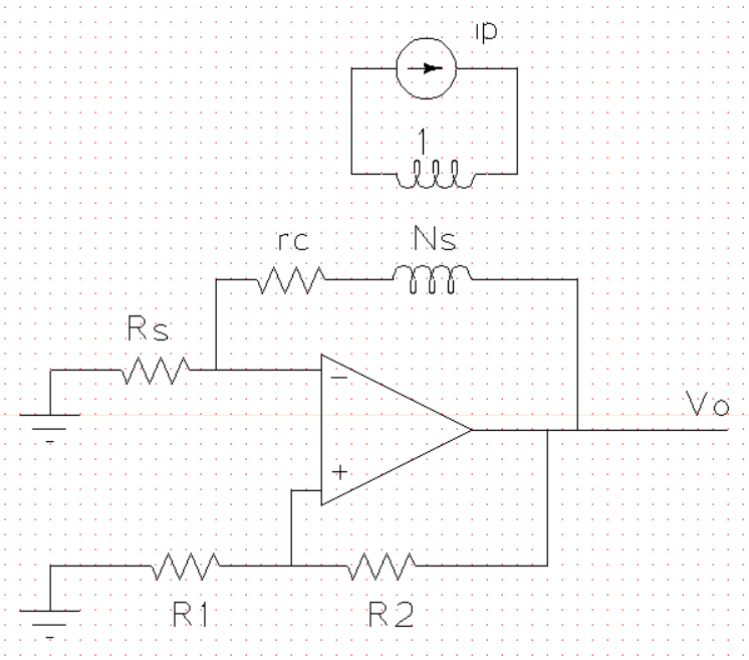

Figure II.7. Excitation and comparator circuit structure.

In Figure II.7, resistors R_1 and R_2 are used to generate the threshold voltage. R_s symbolizes the measurement resistance, while R_c symbolizes the winding resistance. Here the resistance R_s is a very high value compared to R_c. Therefore, the R_c resistance can be neglected. The level of the R_s resistance is usually 4-6 Ohms. The second harmonic component of the excitation current measured across resistance R_s gives an output proportional to the measured residual current. The second harmonic component is detected by demodulating the current in question. However, this method requires processing power and increases the circuit cost. An easier

detection method is to detect the asymmetry in the excitation of the circuit in case of residual current. Normally there is a square wave with a 50% duty cycle, but this ratio changes with the flow of the residual current. Residual current can also be detected in this way. Considering the variables shown in Figure (II.2), the disturbance rate is calculated as shown in Equation (II.1).

$$D = \frac{1}{2} + \frac{(R_s + R_c) \cdot I_p}{2 \cdot V_o \cdot N_s} \tag{II.1}$$

As can be seen from Equation (II.1), the amount of residual current changes the width of the excitation voltage in the circuit. Increasing the secondary winding reduces the sensitivity of the circuit. The linearity of the circuit can be disrupted under certain conditions. In this case, a second winding is added to the toroid. The second winding is called the compensation winding and some current is flowed through the winding to zero the net flux. This provides compensation and increases the linearity and precision of the circuit. The optimum point between high precision and linearity must be found. Otherwise, a structure with very good linearity is problematic in terms of precision.

Before the sensor structure is finalized, the offset drift and input noise of the comparator used must be considered. Otherwise, the stability of the sensor's duty cycle value becomes problematic. As is well known, comparators are good amplifiers for their own noise. Therefore, extra measures must be taken to minimize the input noise.

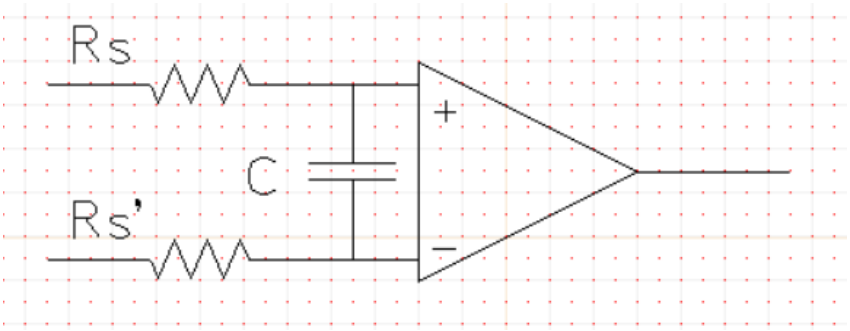

Figure II.8. Noise reduction method.

To obtain a noise-free comparator output, a capacitor (denoted by C in Figure II.8) is placed at the input to improve the circuit performance. The important point here is to choose the value of the capacitor as “small enough”. In practice, this value varies between 100 pF and 1 nF. The type of resistors used in the comparator inputs is also important. Choosing carbon, tin-oxide, and metal film resistors with minimal inductive effects positively affects the circuit performance. An Inductively wound resistor is not a suitable choice.

The break time of an RCD is affected by various design factors, such as the type of magnetic core, the number of turns in the coil, and the shape and size of the magnetic field. The type of magnetic core used in an RCD affects its magnetic field, which in turn affects its break time. There are some RCDs with different types of magnetic cores, including toroidal, U-shaped, and EI-shaped cores. The researchers found that RCDs with toroidal magnetic cores had faster break times than RCDs with other types of cores. This is because toroidal cores have a more uniform magnetic field that allows for faster and more accurate detection of current imbalances. The number of turns in the coil also affects the magnetic field and, therefore, the break time of an RCD. The study found that RCDs with a smaller number of turns in the coil had faster break times than RCDs with a larger number of turns. This is because a smaller number of turns in the coil results in a stronger magnetic field, which allows for faster and more accurate detection of current imbalances. For these reasons, a toroid with a specially selected B-H curve and inductance value is designed. The designed toroid is analyzed by using ANSY Maxwell. Figure (II.9a) shows the designed toroid. Figure (II.9b) presents the H distribution of the designed toroid for 30 mA analysis results. Figure (II.9c) presents the J distribution of the designed toroid for 30 mA analysis results. Figure (II.9d) presents the H distribution of the designed toroid for the 6 mA analysis results. Figure (II.9e) presents the J distribution of the designed toroid for 6 mA analysis results.

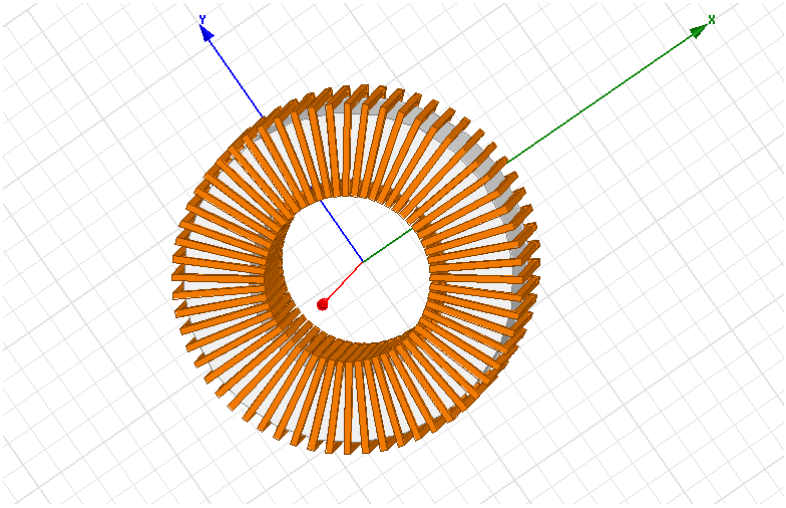

(a)

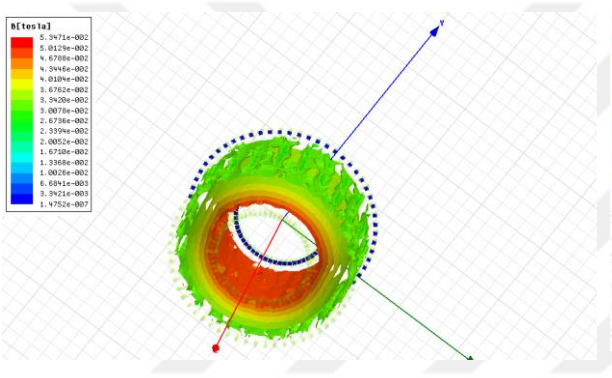

(b)

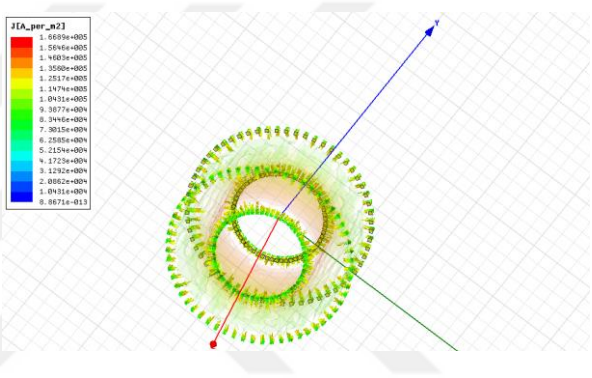

(c)

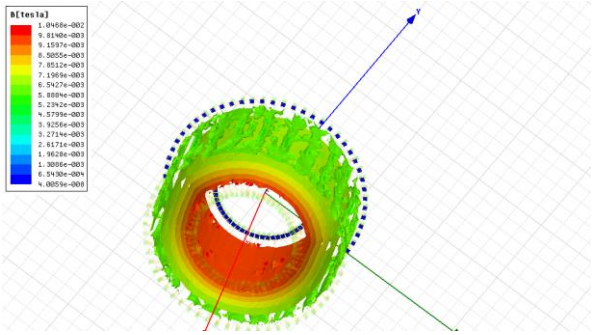

(d)

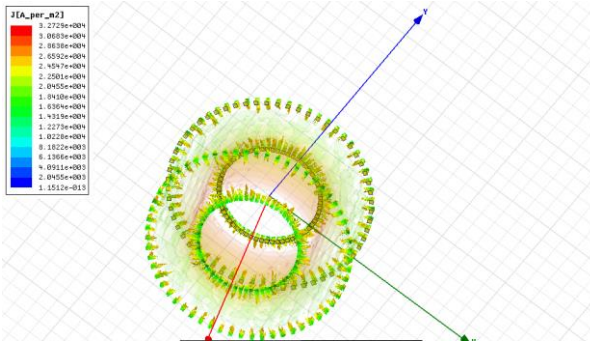

(e)

Figure II.9. ANSYS Maxwell design results, (a) View of the designed toroid, (b) 30 mA AC analysis result (Distribution B), (c) 30 mA AC analysis result (Distribution J), (d) 6 mA DC analysis result (Distribution B), (e) 6 mA DC analysis result (Distribution J).

The results of the analysis demonstrated the fabrication parameters of a toroid made of soft material with high permeability for the detection of AC and DC signal variations within a range of 0-30 mA. Although the toroids available in the market are made of ferrite material, the toroid produced is made of an alloy metal material. The primary winding inductance value of the manufactured toroid is measured as 410 mH and the secondary winding value as 210 µH. The selection of the magnetic core is important for the sensor's performance. The core material and dimensions should also allow for low-amplitude excitation current generated by a low-power electronic circuit. Increasing the number of turns in the excitation coil can reduce the required excitation current, but it also increases non-saturated inductance, which affects the excitation current frequency. A high coil inductance results in reduced bandwidth and slow transient response, which must be addressed for low noise output voltage.

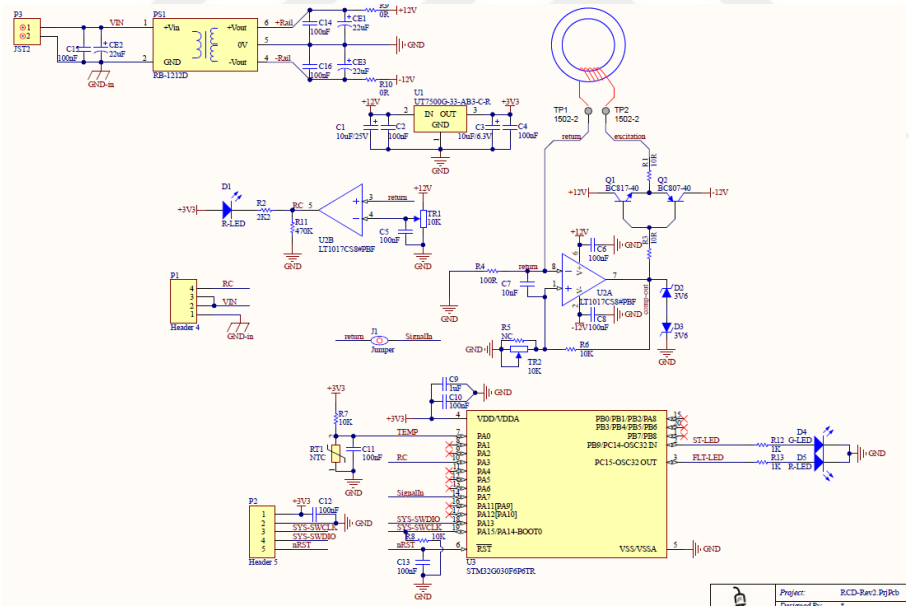

Figure II.10. Circuit schematic of the developed prototype.

Figure (II.10) shows the circuit diagram of the developed prototype. STM32G030F6P6TR processor is used to increase communication and digital signal processing capability. The excitation winding is reduced to one in the circuit. Circuit designs are realized by using the Altium software.

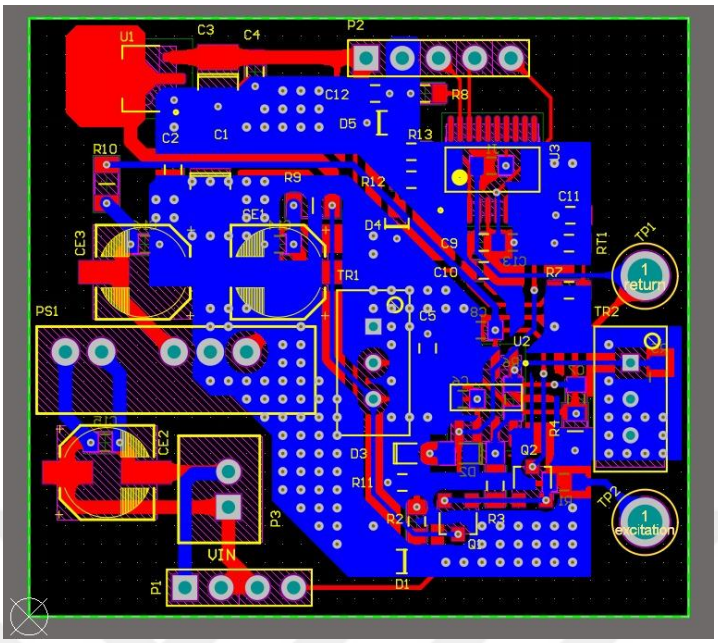

Figure II.11. PCB design of the developed prototype.

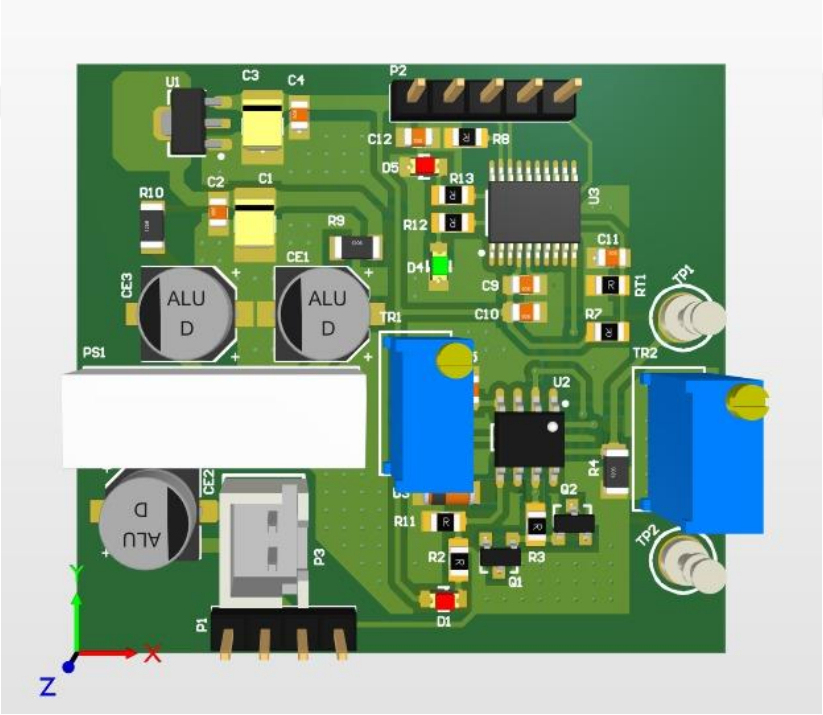

Figure II.12. PCB design view of the developed prototype (top view).

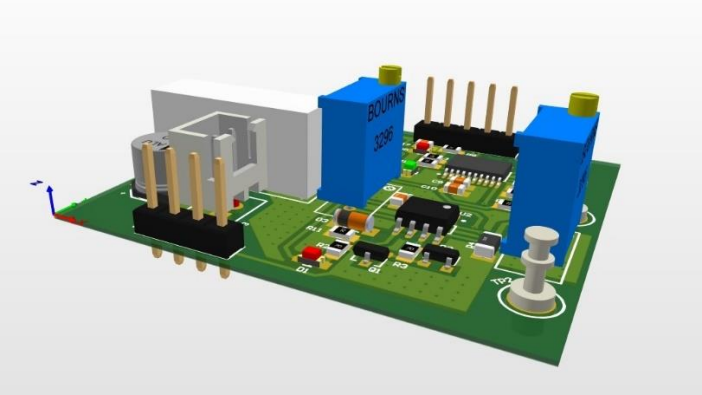

Figure II.13. PCB design view of the developed prototype (side view).

Figure (II.11) shows the top surface design of the PCB design of the prototype. Figures (II.12) and (II.13) show the final PCB view by importing the three-dimensional views of the materials into the Altium software.

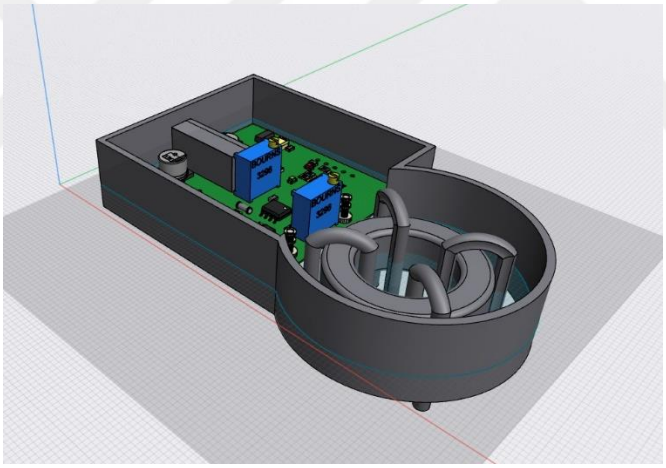

Figure II.14. CAD design of the developed prototype.

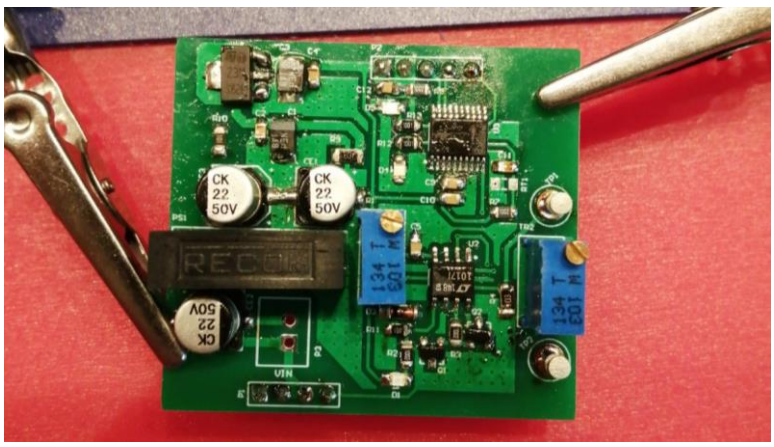

Figure II.15. Assembled version of the developed prototype.

Figure (II.14) shows the mechanical designed in Solidworks software. There are two types of mechanical design approaches for residual current sensors. In the first one, the phase cables connect directly through the toroid, and in the second one, the mechanical structure which keeps the phase cables outside can be mounted directly on the PCB. Within the scope of the thesis, a mechanical assembly has been designed where the phase cables are kept outside, by considering the trends of todays. Figure (II.15) shows the printed-circuit board produced. Figure (II.16) shows the fully assembled residual current sensor.

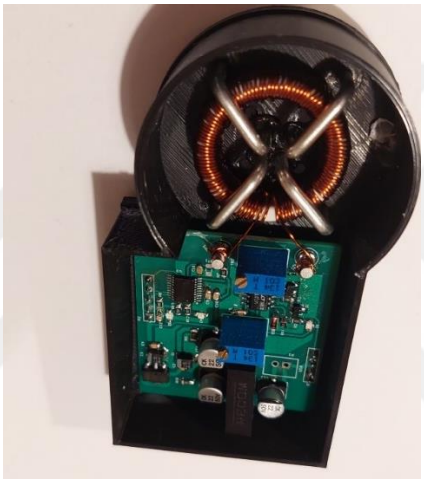

Figure II.16. Assembled version of the developed prototype.

III. EXPERIMENTAL STUDIES

Within the scope of the experimental studies of the residual current sensor, whose design and manufacturing stages are presented in Section II, the printed-circuit board of an electric vehicle charging equipment manufacturer company in Turkey is redesigned and manufactured according to the residual current sensor manufactured within the scope of the thesis. Figure (III.1) and Figure (III.2) show the integration of portable charging equipment and the residual current sensor produced within the scope of the thesis. AC EVSE is the equipment used to supply electrical energy to an electric vehicle for charging its battery. The safety of the AC EVSE is crucial for the safe operation of electric vehicles. The safety standards and regulations for AC EVSE is IEC 61851 and UL 2231 standards. These standards specify the safety requirements for AC EVSE, such as protection against electric shock, overcurrent protection, and protection against short circuits. The safety standards for EV charging systems aim to minimize the risk of danger to users and surroundings. This involves protecting against electric shock, fire hazards, and injury hazards. The protection system includes insulation and protective devices, such as overvoltage and overcurrent protection devices, residual current devices (RCDs), residual current monitoring, and charging interrupting devices. An RCD is used to detect residual current and disconnect the power line circuit when a fault occurs. To reduce the risk of leakage current, the EVSE should be protected by an RCD with a rated residual operating current not exceeding 30 mA and should be at least type A. An EVSE equipped with a vehicle connector requires protective measures against DC fault current by using an RCD type B or RCD Type A with additional equipment to disconnect the supply if DC fault current above 6 mA is detected. This protection is important because charging EV's battery involves power converter devices such as a rectifier and/or inverter.

The design includes a control module, a communication module, a power module, and a protection module. The control module is responsible for controlling the charging process, while the communication module enables communication with the electric vehicle. The power module converts the AC power supply to DC power for charging the battery, and the protection module provides safety features such as overcurrent protection and protection against short circuits. Designing AC EVSE based on safety standards is essential for ensuring the safety of electric vehicles and their users. The proposed design provides a comprehensive solution for AC EVSE, incorporating safety features and compliance with safety standards and regulations. The testing and certification process ensures that the AC EVSE is safe to use and can be trusted by electric vehicle owners.

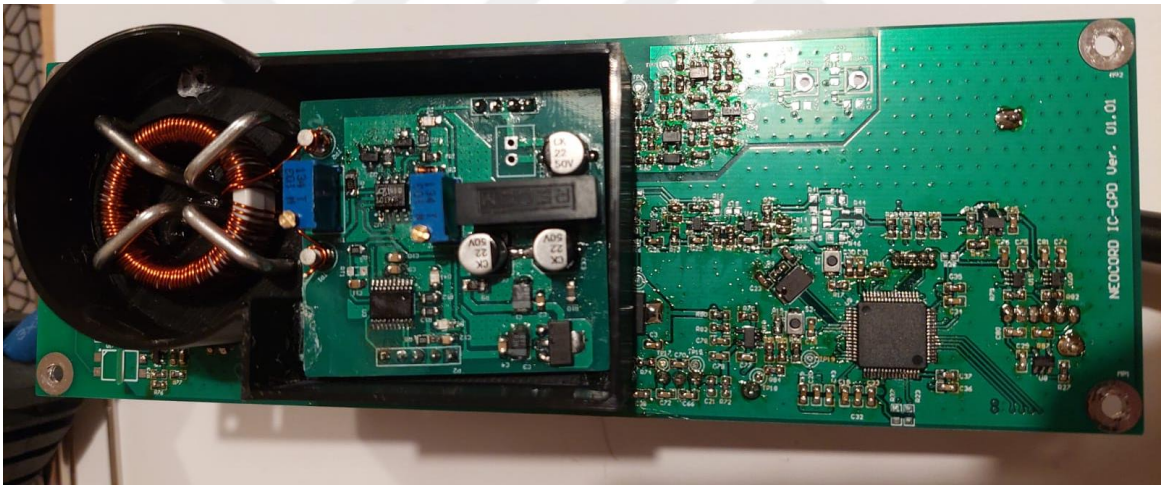

Figure III.1. Test circuit integrated into a commercially available product for on-vehicle testing.

Within the scope of the thesis, on-vehicle tests are conducted on a BMW i3 vehicle with the equipment shown in Figure (III.1) Test results are presented in Figures (III.2) - (III.5). Figure (III.2) shows 6 mA DC residual current, Figure (III.3) shows 13 mA DC test result and Figure (III.4) shows 15 mA DC residual current detection test result. Figure (III.5) shows the 30 mA AC test result. The DC shown in red in Figure (III.2) - (III.4) shows a square wave signal whose width increases with residual current. The microcontroller detects the amplitude of this square

wave, calculates the residual current value accordingly, and generates the error signal. In this figure, a residual current of 6 mA is flowed at around 100 ms and the amplitude of the square wave increased at around 500 ms. The self-oscillation frequency of the circuit is approximately 17 Hz. This shows that residual current can be detected within 7 periods. Detection became even easier when the residual current value is increased to 13 mA. The residual current reached a detectable level at approximately 5 periods (300 ms). There is a detection time of 4 periods (240 ms), when a DC residual current of 15 mA occurs. AC residual current is relatively easy to detect. The structure is designed to generate a pulse every 150 ms, when a residual current of 30 mA (RMS) at a frequency of 50 Hz occurs in the circuit. Since the residual current is detected via a rectified signal, a signal frequency proportional to the flowing residual current is obtained at this point.

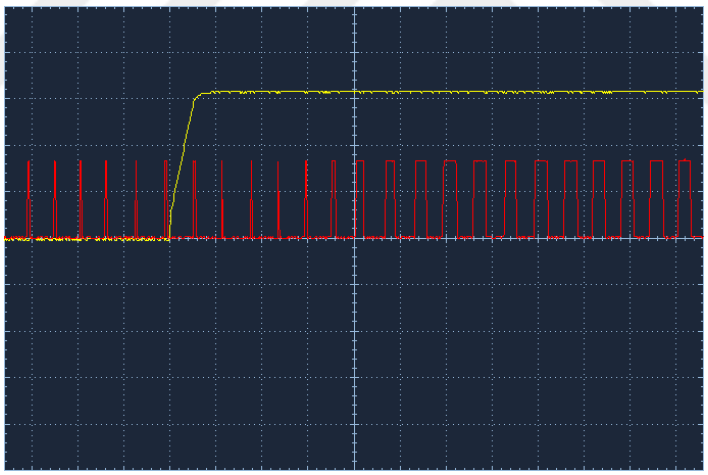

Figure III.2. 6 mA DC test result (Yellow: 2mA/div, Red: 2V/div, Time: 100 ms/div).

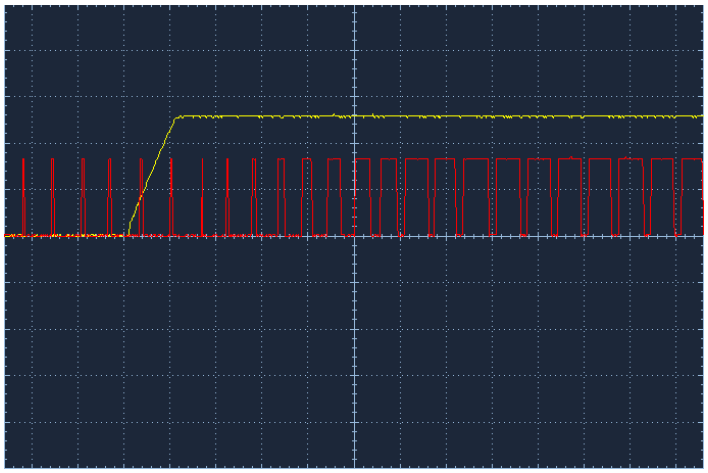

Figure III.3. 13 mA DC test result (Yellow: 5mA/div, Red: 2V/div, Time: 100 ms/div).

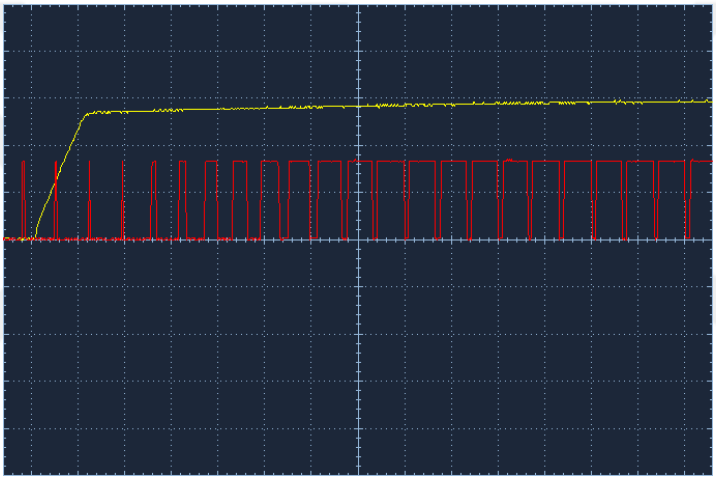

Figure III.4. 15 mA DC test result (Yellow: 5mA/div, Red: 2V/div, Time: 100 ms/div).

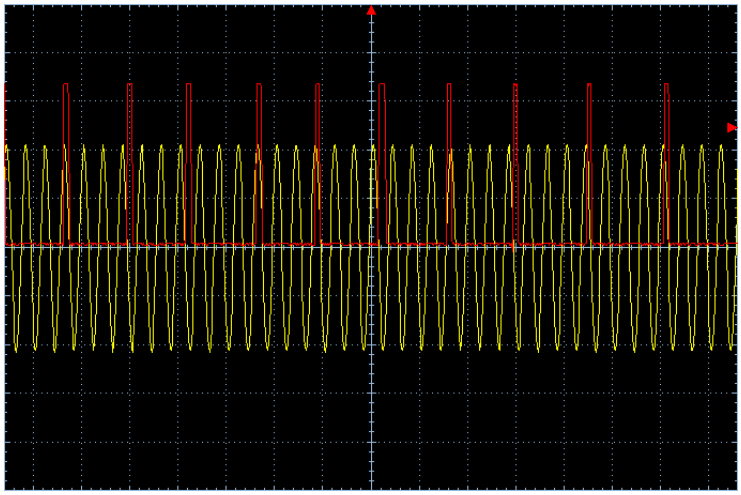

Figure III.5. 30 mA AC test result (Yellow: 20mA/div, Red: 1V/div, Time: 50 ms/div).

VI. CONCLUSION

With the proliferation of electric vehicle charging equipment and stations (Mode 2 and Mode 3), AC and DC residual current detection has become mandatory as per the IEC62752 standard. As a result of this necessity, a limited number of companies develop residual current sensors. Within the scope of the thesis, an RCD sensor is designed, developed and manufactured. The original approach of the residual current sensor developed within the scope of the thesis is presented in Figure (II.10). In summary, in the circuit developed in the thesis, transistors (Q_1) and (Q_2) are designed as a common emitter amplifier. A resistor (R_1) is connected to the line to limit the winding current. The output of the comparator (U_2) is taken into the integrated circuit via a voltage divider. This comparator ensures the operation of the self-oscillating circuit. (D_2) and (D_3) zener diodes are added to limit the output voltage. The return line of the winding terminates on resistor (R_4) and the voltage signal enters the negative terminal of the comparator. To improve the stability performance of the comparator, a small value capacitor is added between ± pins. The signals obtained are processed on the microprocessor and the error output is transmitted to the charging equipment. RCDs with toroidal magnetic cores, a smaller number of turns in the coil, and a more uniform magnetic field are more efficient and provide faster protection. Within the scope of the thesis, toroid design is designed using ANSYS Maxwell, circuit design with Altium, and mechanical design with Solidworks. As a result of the experimental studies on the electric vehicle, high-resolution DC and AC residual currents are detected and the circuit is successfully interrupted. Thus, for the first time at the national level, a residual current sensor that meets the IEC 62752 standard requirements has been developed and its preliminary prototype tests are completed. As a result of the experimental studies, the developed system is verified for 6 mA DC, 30 mA AC residual current.

REFERENCES

[1] D. Cheng, B. Zhang, S. Xiong, Z. Xie and Z. Xue, “Residual Current Detection Prototype and Simulation Method in Low Voltage DC System,” in IEEE Access, vol. 10, pp. 51100-51109, 2022.

[2] S. Czapp, H. Tariq, S. Cieslik, “Behavior of Residual Current Devices at Earth Fault Currents with DC Component”, in Sensors 2022, 22, 8382.

[3] International Energy Agency (IEA),” Global EV Outlook 2021”, Technology report. April 2021 [Online] Available: https://www.iea.org/reports/global-ev-outlook-2021.

[4] T. R. Oliveira, "Design of a Low-Cost Residual Current Sensor for LVDC Power Distribution Application," 2018 13th IEEE International Conference on Industry Applications (INDUSCON), São Paulo, Brazil, 2018, pp. 1313-1319.

[5] Henry S. Chung; Yuanbin He; Min Huang; Weimin Wu; Frede Blaabjerg, "Control Structure and Modulation Techniques of Single-Phase Grid-Connected Inverter," in Control and Filter Design of Single-Phase Grid-Connected Converters, IEEE, 2023, pp.29-41.

[6] N. Ahmed and Z. R. Khan, "A Single-Phase Grid-Connected Inverter using Phase Control Method," 2021 IEEE International Conference in Power Engineering Application (ICPEA), Malaysia, 2021, pp. 183-187.

[7] A. Hota, V. Sonti, S. Jain and V. Agarwal, "Common Mode Voltage Elimination in Single-Phase Multilevel Inverter using a 3rd Leg," 2021 International Conference on Sustainable Energy and Future Electric Transportation (SEFET), Hyderabad, India, 2021, pp. 1-5.

[8] Zhiguo Lu, Chunjun Wu, Lili Zhao and Wanping Zhu, "A new three-phase inverter built by a low-frequency three-phase inverter in series with three high-frequency single-phase inverters," Proceedings of the 7th International Power Electronics and Motion Control Conference, Harbin, 2012, pp. 1573-1577.

[9] T. Qanbari and B. Tousi, "Single-Source Three-Phase Multilevel Inverter Assembled by Three-Phase Two-Level Inverter and Two Single-Phase Cascaded H-Bridge Inverters," in IEEE Transactions on Power Electronics, vol. 36, no. 5, pp. 5204-5212, May 2021.

[10] Dehong Xu; Rui Li; Ning He; Jinyi Deng; Yuying Wu, "Soft-switching SiC Three-phase Grid Inverter," in Soft-Switching Technology for Three-phase Power Electronics Converters, IEEE, 2022, pp.321-369.

[11] M. I. Haq, J. T. Humayra, M. Rahman, S. Tanzil and A. H. Hanan, "Control and Simulation of a Three-Phase Inverter," 2021 IEEE Conference of Russian Young Researchers in Electrical and Electronic Engineering (ElConRus), St. Petersburg, Moscow, Russia, 2021, pp. 1419-1424.

[12] M. Anzari, J. Meenakshi and V. T. Sreedevi, "Simulation of a transistor clamped H-bridge multilevel inverter and its comparison with a conventional H-bridge multilevel inverter," 2014 International Conference on Circuits, Power and Computing Technologies [ICCPCT-2014], Nagercoil, India, 2014, pp. 958-963.

[13] A. S. Mohamad, "Matrix Inverter: A Multilevel Inverter Based on Matrix Converter Switch Matrix," 2020 IEEE Electric Power and Energy Conference (EPEC), Edmonton, AB, Canada, 2020, pp. 1-5.

[14] S. S. Barah and S. Behera, "An Optimize Configuration of H-Bridge Multilevel Inverter," 2021 1st International Conference on Power Electronics and Energy (ICPEE), Bhubaneswar, India, 2021, pp. 1-4.

[15] Kamel, R.M.; Chaouachi, A.; Nagasaka, K. Comparison the performances of three earthing systems for micro-grid protection during the grid connected mode. Smart Grid Renew. Energy 2011, 2, 206–215.

[16] H. Mafi, R. Yared and L. Bentabet, "Smart Residual Current Circuit Breaker with Overcurrent protection," 2019 IEEE 2nd International Conference on Renewable Energy and Power Engineering (REPE), Toronto, ON, Canada, 2019, pp. 6-9.

[17] K. Fahem, D. E. Chariag and L. Sbita, "On-board bidirectional battery chargers' topologies for plug-in hybrid electric vehicles," 2017 International Conference on Green Energy Conversion Systems (GECS), Hammamet, Tunisia, 2017, pp. 1-6.

[18] A. N. Ravishankar, S. Kumaravel and S. Ashok, "Bidirectional Dual Input Single Output DC-DC Converter for Electric Vehicle Charger Application," 2019 IEEE 8th Global Conference on Consumer Electronics (GCCE), Osaka, Japan, 2019, pp. 85-86.

[19] A. H. AlMarzoogee and A. H. Mohammed, "Design a Bidirectional DC/DC Converter for Second-Level Electric Vehicle Bidirectional Charger," 2020 4th International Symposium on Multidisciplinary Studies and Innovative Technologies (ISMSIT), Istanbul, Turkey, 2020, pp. 1-3.

[20] N. Wang et al., "Self-Oscillating Fluxgate-Based Quasi-Digital Sensor for DC High-Current Measurement," in IEEE Transactions on Instrumentation and Measurement, vol. 64, no. 12, pp. 3555-3563, Dec. 2015.

[21] I. M. Filanovsky and V. A. Piskarev, "Sensing and measurement of DC current using a transformer and RL-multivibrator," IEEE Trans. Circuits Syst., vol. 38, no. 11, pp. 1366–1370, Nov. 1991.

[22] I. M. Filanovsky and V. A. Piskarev, “RL-multivibrator and retrieving the coil magnetization curve,” IEEE Trans. Circuits Syst., vol. 38, no. 6, pp. 650–653, Jun. 1991.

[23] A. Pross, C. Lewis, and T. Hesketh, “A low cost analogue current transducer,” Sens. Actuators A, Phys., vol. 76, nos. 1–3, pp. 72–77, 1999.

[24] M. M. Ponjavic and R. M. Duric, “Nonlinear modeling of the self-oscillating fluxgate current sensor,” IEEE Sensors J., vol. 7, no. 11, pp. 1546–1553, Nov. 2007.

[25] X. Zeliang, M. Yingzong, D. Feng, Z. Yue, and M. Anheuser, “Type B RCD with a simplified magnetic modulation/demodulation method,” in Proc. IEEE 6th Int. Power Electron. Motion Control Conf., May 2009, pp. 769–772.

[26] M. Yingzong, D. Feng, C. Weigang, Z. Yue, and M. Anheuser, “An AC/DC sensing method based on adaptive magnetic modulation technology with double feedback properties,” in Proc. IEEE Int. Workshop Appl. Meas. Power Syst. (AMPS), Sep. 2011, pp. 48–52.

[27] P. Pejovi´c, “A simple circuit for direct current measurement using a transformer,” IEEE Trans. Circuits Syst. I, Fundam. Theory Appl., vol. 45, no. 8, pp. 830–837, Aug. 1998.

[28] R. Duric and M. Ponjavic, “Self-oscillating fluxgate current sensor with pulse width modulated feedback,” Electronics, vol. 14, no. 2, p. 33, 2010.

[29] E. Hashiguchi, T. Koseki, E. Favre, M. Ashiya, and T. Tachibana, “Nonlinear magnetic circuit analysis of fluxgate current sensor,” in Proc. 12th Int. Symp. Interdiscip. Electromagn., Mech. Biomed. Problems, 2005, pp. 76–77.

[30] T. Koseki, Y. Takada, H. Obata, Y. Hayakeyama, W. Teppan, and E. Favre, “Measurement and modeling of nonlinear magnetic core characteristics of a

fluxgate direct current sensor for wide-range current monitoring," in Proc. Int. Conf. Elect. Mach. Syst., Nov. 2009, pp. 1–6.

[31] T. Kudo, S. Kuribara, and Y. Takahashi, "Wide-range ac/dc earth leakage current sensor using fluxgate with self-excitation system," in Proc. IEEE Sensors, Oct. 2011, pp. 512–515.

[32] BMW Group. 2017. "ISO15118 Standardization and Market Introduction".

[33] Czapp, S. 2008. "The Impact of DC Earth Fault Current Shape on Tripping of Residual Current Devices", Elektronika ir Elektrotechnika, 9-12.

[34] Czapp, S., etc. 2017. "Improving Sensitivity of Residual Current Transformers to High Frequency Earth Fault Currents", Arch. Elect. Eng., 485-494.

[35] Freschi, F. 2012. "High-Frequency Behavior of Residual Current Devices", IEEE Trans. Power Deliv, 1629-1635.

[36] Grand View Research. 2017. "Electric Vehicle (EV) Charging Infrastructure Market Analysis by Charger Type (Slow Charger, Fast Charger), By Connector (CHAdeMO, Combined Charging System), By Application, By Region, And Segment Forecasts, 2018 – 2025".

[37] IEC. 2016. "In-cable control and protection device for mode 2 charging of electric road vehicles (IC-CPD)".